Journal of Dentistry 134 (2023) 104521

Contents lists available at ScienceDirect

Journal of Dentistry

journal homepage: www.elsevier.com/locate/jdent

Influence of type of restorative materials and surface wetness conditions on intraoral scanning accuracy

Rubén Agustín-Panadero [a], David Macías Moreno [b], Jorge Alonso Pérez-Barquero [c], Lucía Fernández-Estevan [c], Miguel Gómez-Polo [d,*], Marta Revilla-León [e,f,g]

[a] Department of Stomatology, School of Medicine and Dentistry, University of Valencia, Valencia, Spain
[b] Private Practice, Valencia, Spain
[c] Department of Dental Medicine, Faculty of Medicine and Dentistry, University of Valencia, Valencia, Spain
[d] Department of Conservative Dentistry and Prosthodontics, Director of Postgraduate Program of Advanced in Implant-Prosthodontics, School of Dentistry, Complutense University of Madrid, Madrid 28033, Spain
[e] Department of Restorative Dentistry, School of Dentistry, University of Washington, Seattle, WA, United States
[f] Faculty & Director of Research and Digital Dentistry, Seattle, WA, United States
[g] Department of Prosthodontics, School of Dental Medicine, Tufts University, Boston, MA, United States

ARTICLE INFO

Keywords:
Accuracy
Digital impression
Humidity
Intraoral scanner
Restorative dental materials
Wetness

ABSTRACT

Objectives: To assess the influence of different restorative materials and surface wetness on intraoral scanning accuracy.
Methods: Reference casts with an extracted second premolar and first and second molar were digitized (L2). Four groups were established according to the material of the first molar: natural tooth (control), zirconia (Z), lithium disilicate (LD), and nanoceramic resin crown (NC). Four subgroups were developed: dry, low-, mild-, and high-wetness subgroups ($n = 15$). All the scans were completed by using an intraoral scanner (TRIOS 3). In the control-dry subgroup, the reference cast was dry. In the control-low subgroup, artificial saliva was sprayed with a 1 mL/min volumetric flow for 4 s. In the control-mild and control-high subgroups, the same procedures as in the control-low subgroup were performed, but with a volumetric flow of 4 and of 8 mL/min, respectively. In the Z, LD and NC groups, each crown was fabricated with its respective material. Trueness was analyzed using 2-way ANOVA and Bonferroni tests. The Levene and Bonferroni tests were used to assess precision ($\alpha = 0.05$).
Results: Material ($P < .001$) and wetness ($P < .001$) significantly influenced trueness and precision. The mild and high subgroups revealed lower trueness and precision compared with the dry and low subgroups. The control, Z, and LD groups under dry and low wetness conditions showed better trueness compared with the NC group, but the materials tested had no significant precision discrepancies. Under mild wetness conditions, all the materials showed no significant trueness discrepancies. Under high wetness conditions, the LD group demonstrated the best trueness and precision.
Conclusions: The restorative materials and surface wetness tested influenced scanning trueness and precision of the IOS assessed.
Clinical significance: Dried surfaces are recommended to maximize the scanning accuracy values of the IOS tested. Overall, the presence of saliva and dental restorations can reduce the performance of the IOS tested.

1. Introduction

The use of intraoral scanners (IOSs) for performing a range of dental procedures has grown steadily in recent years, due to continuous improvements of the systems, as well to improved knowledge of the influencing factors related to operator skills and decisions and the intraoral conditions of the patient being digitized [1–7]. These factors include the scanning technology [8,9], ambient temperature changes [10], scanning pattern [11,12], length of the digital scan [13,14], previous experience handling IOSs [15–17], ambient lighting settings [18–20], characteristics of the surface being scanned [21–24], and cutting-off and rescanning techniques [25,26]. When dental implants

* Corresponding author.
E-mail address: mgomezpo@ucm.es (M. Gómez-Polo).

https://doi.org/10.1016/j.jdent.2023.104521
Received 18 December 2022; Received in revised form 26 March 2023; Accepted 12 April 2023
Available online 13 April 2023

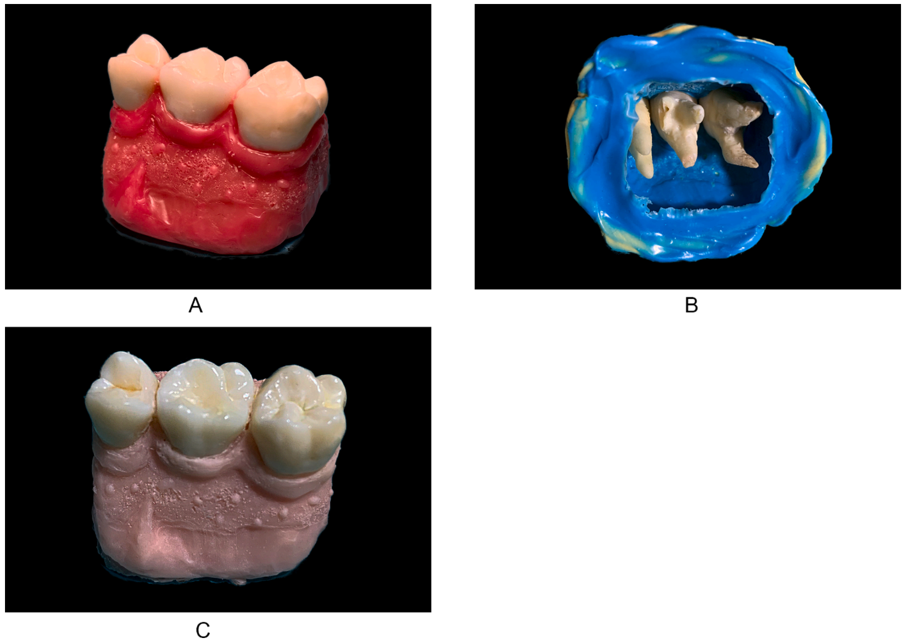

Fig. 1. A, Extracted human teeth contained in a waxed-up base. B, Extracted teeth positioned in the polyvinyl siloxane impression. C, Reference cast.

are present, additional factors should be considered, including the implant scan body design [27,28] and implant position [29–34].

The presence of existing restorations on the dentition being digitized has been reported as an element that can reduce the scanning accuracy of IOSs [35,36]. The different reflective behavior of the restorative materials compared with the dental hard tissues affects scanning accuracy differently, depending on the IOS technology used [35,36]. Additionally, glazed restorations seem to have a greater impact upon the scanning performance of IOSs than polished dental restorations [36].

The wetness characteristics of the surface being digitized by using IOSs have been identified as a factor that may affect intraoral scanning accuracy; however, these studies reported contradictory results [37–41]. Some studies have reported that wetness of the surface being digitized decreased scanning accuracy of the IOSs tested [37,38,41], while another study concluded that the IOSs tested were not sensitive to humid environmental conditions [39]. Hence, the influence of the wetness characteristics of the surface being scanned on intraoral scanning accuracy remains unclear.

The purpose of the present in vitro study was to evaluate the influence of restorative materials (natural tooth, zirconia, lithium disilicate, and nanoceramic resin material) and wetness characteristics of the surface being digitized (dry, low, mild, and high wetness) on intraoral scanning accuracy. The null hypothesis was that there would be no significant difference in scanning accuracy (trueness and precision) of the IOS system tested among the digital scans obtained with varying restorative materials and surface humidity conditions tested.

2. Materials and methods

The protocol of this *in vitro* study was approved by the Institutional Review Board (IRB) (IRB-1910025). The inclusion criteria involved maxillary or mandibular molar and premolar teeth that were planned to be extracted due to different reasons, such as orthodontic or periodontal management. The teeth were intact without any existing restoration or dental caries. A total of 2 molars and 1 premolar were obtained. The extracted teeth were cleaned and maintained in saline solution.

A cast with 3 extracted human teeth was created. The 3 teeth included were a maxillary left second premolar and first and second molar. Firstly, the 3 teeth were aligned and positioned in a waxed-up base (Modelling Wax; Cera Reus) aiming to replicate the intraoral tissue contours (Fig. 1A). Subsequently, a polyvinyl siloxane impression (Elite HD Zhermack) was obtained using a custom tray (Triad Tru Tray; VLC) following the manufacturer's recommendations. Then, the extracted teeth were removed from the waxed-up based and positioned into the impression (Fig. 1B). Lastly, the impression was poured by using autopolymerizing acrylic resin material (Pink Acrylic Resin; Sintodent). After the complete the polymerization of the material, the reference cast was obtained (Fig. 1C).

The reference cast was digitized by using a laboratory scanner (L2 scanner; Imetric 4D) following the manufacturer's recommendations. The scanner was previously calibrated by using the protocol endorsed by the manufacturer. The reference scan for the control group was exported in a standard tessellation language (STL) file format. The manufacturer of the scanner reports a scanning trueness of <5 μm and a precision of <10 μm [18].

Four groups were established according to the surface material of the maxillary first molar of the reference cast: natural tooth (control group), zirconia (Z group), lithium disilicate ceramic (LD group), and a nanoceramic resin material (NC group). Additionally, each group was divided into 4 subgroups based on the wetness conditions created before acquiring the intraoral digital scans: dry (dry subgroup), low (low subgroup), mild (mild subgroup), and high (high subgroup) ($n = 15$). All the intraoral digital scans were completed by using an IOS (TRIOS 3, pod; 3Shape A/S) in a room at constant temperature (24 ± 2 °C), relative humidity of 55%, [10] and at 1000-lux ambient lighting conditions (LX1330B Light Meter; Dr. Meter Digital Illuminance) following the recommended scanning protocol [18–21]. The IOS was calibrated before starting the experiment and each time the subgroup was changed, using the calibration devices and calibration protocol endorsed by the manufacturer [10]. Furthermore, the same experienced prosthodontist acquired all the intraoral digital scans of the study, with a 30 min resting period every 10 scans in order to avoid operator fatigue. The operator had 10 years of previous experience handling IOSs.

The sample size was determined considering the results of a pilot study performed by the authors of this study. The power analysis (G*Power 3.1.9.4; University of Kiel, Kiel, Germany) showed $n = 15$ to be sufficient to detect 10% of mean RMS error values discrepancies with 75.3% statistical power and a 95% confidence level.

In the control-dry subgroup, the dry reference cast was consecutively digitized by using the selected IOS following the scanning protocol

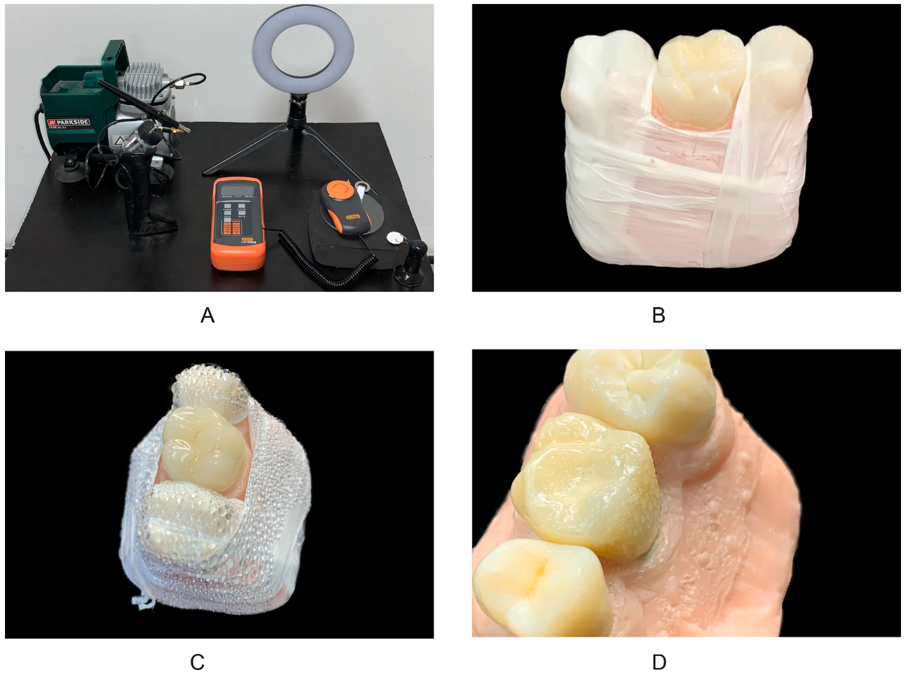

Fig. 2. Representative setting for the low, mild, and high wetness subgroups. A, Scanning setup composed of an automated rotatory platform with a stop magnet system and an airbrush under standardized ambient temperature and lighting conditions. Airbrush system equipped with an air compressor and nebulizer. B, Isolated maxillary first molar using Teflon tape. C, After the nebulization procedure. D, Surface wetting detail after Teflon tape removal.

Table 1
Main characteristics of the subgroups tested.

Group	Subgroup	Surface of the first molar being scanned	Surface wetness conditions (artificial saliva)
Control	Dry	Enamel of the intact extracted human tooth	Dry
	Low		1 mL/min for 4 s
	Mild		4 mL/min for 4 s
	High		8 mL/min for 4 s
Z	Dry	Zirconia (IPS e.max ZirCad; Ivoclar Vivadent)	Dry
	Low		1 mL/min for 4 s
	Mild		4 mL/min for 4 s
	High		8 mL/min for 4 s
LD	Dry	Lithium disilicate ceramic (IPS e.max CAD; Ivoclar Vivadent)	Dry
	Low		1 mL/min for 4 s
	Mild		4 mL/min for 4 s
	High		8 mL/min for 4 s
NC	Dry	Nanoceramic resin (Grandio; VOCO)	Dry
	Low		1 mL/min for 4 s
	Mild		4 mL/min for 4 s
	High		8 mL/min for 4 s

LD, lithium disilicate; NC, nanoceramic resin; Z, zirconia.

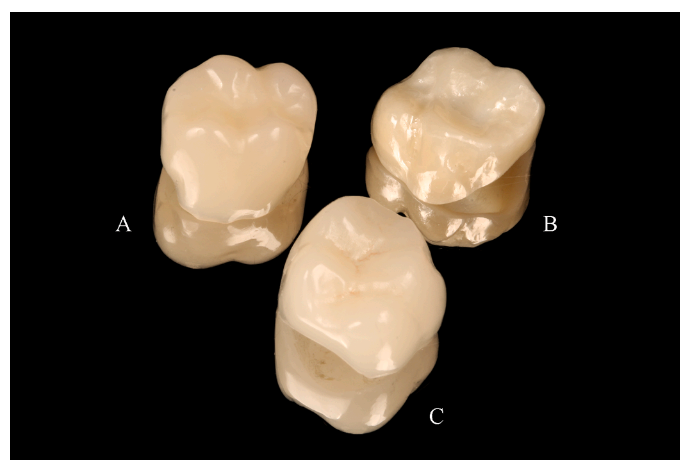

Fig. 3. Maxillary crowns fabricated for the first molar of the reference cast. A, Zirconia (Z group). B, Lithium disilicate ceramic (LD group). C, Nanoceramic resin material (NC group).

recommended by the manufacturer. The intraoral digital scan started at the occlusal surface of the second molar and continued anteriorly towards the occlusal surface of the second premolar. Then, the scan continued towards the buccal surfaces from the second premolar to the second molar. Lastly, the lingual area was digitized from the second molar to the second premolar. The intraoral digital scans were acquired without leaving mesh holes [25,26]. Each intraoral digital scan was postprocessed automatically by the IOS software program and exported in STL file format ($n = 15$).

A customized airbrush system was developed to recreate standardized humidity surface conditions for the low, mild, and high wetness subgroups (Fig. 2A). The system consisted of an automatic rotatory platform and an airbrush set. The rotatory platform (Salmueydatgsq4ci-02; Salmune Store) had a magnet system to control the movement of the platform. The rotatory platform was used to facilitate the uniform application of artificial saliva onto the surface of the reference cast. The platform rotated at a speed of 15 rpm. The airbrush system had an air compressor (PABk 60 A1; Parkside) operating at 100 W, 130 V and 50 Hz, with an air flow of 1.5 l/min and a pressure of 0.35–0.15 MPa. The airbrush system was equipped with a nebulizer in which the liquid flow was controlled at 1 mL/min (low subgroup), 4 mL/min (mild subgroup), and 8 mL/min (high subgroup) to standardize the amount of artificial saliva (Spray Moisturizing Biotène; GSK Consumer Healthcare) nebulized on each specimen in each subgroup (Table 1).

In the control-low subgroup, Teflon tape (PTFE plumber tape; William H. Harvey Company) was used to isolate all the reference cast except the first molar aiming to only create wetness on the surface of the

Fig. 4. Assembled reference cast for the Z group. Z, Zirconia.

maxillary first molar (Fig. 2BCD). The reference cast was positioned placed on the automatic rotatory platform with the nebulizer positioned at 15 cm distance and 34° angle in respect to the surface of the rotatory platform. The nebulizer sprayed artificial saliva into the reference cast with a 1 mL/min of volumetric fluid flow for a complete turn of the rotatory platform in 4 s. Subsequently, the Teflon tape was removed, and an intraoral digital scan was captured with the same protocol as in the control-dry subgroup. The digital scan was postprocessed automatically by the IOS software program and exported in STL file format ($n = 15$).

In the control-mild and control-high subgroups, the same procedures as in the control-low subgroup were performed, except for the amount of artificial saliva nebulized onto the first molar of the reference cast. In the control-mild subgroup, a volumetric fluid flow of 4 mL/min during a complete turn of the rotatory platform in 4 s was completed. In the control-high subgroup, a volumetric fluid flow of 8 mL/min during a complete turn of the rotatory platform in 4 s was accomplished.

In the Z, LD, and NC groups, an anatomically contoured and monolithic crown was prepared on each group. In order to fabricate these restorations, the reference cast was first digitized by using an IOS (CEREC Omnicam AC; Dentsply Sirona) following the scanning pattern recommended by the manufacturer. Then, the first molar was prepared for an anatomically contoured crown using a chamfer bur (828.022, KS0, KS1; Komet USA) with a high-speed rotatory instrument under water irrigation. The tooth preparation had a total convergence angle of 10 to 12° and a circumferential chamfer margin of 1 mm. The tooth preparation was digitized by using the same IOS device following the manufacturer's protocol. Lastly, the intraoral digital scans were imported into a CAD software program (CEREC CAD/CAM; Dentsply Sirona) for designing an anatomically contour crown. The initial scan containing the tooth before its preparation was used as a diagnostic waxing to mimic the tooth anatomy into the crown design. The virtual crown design was exported in (STL) file format.

The STL file of the crown design was used to fabricate 3 crowns with

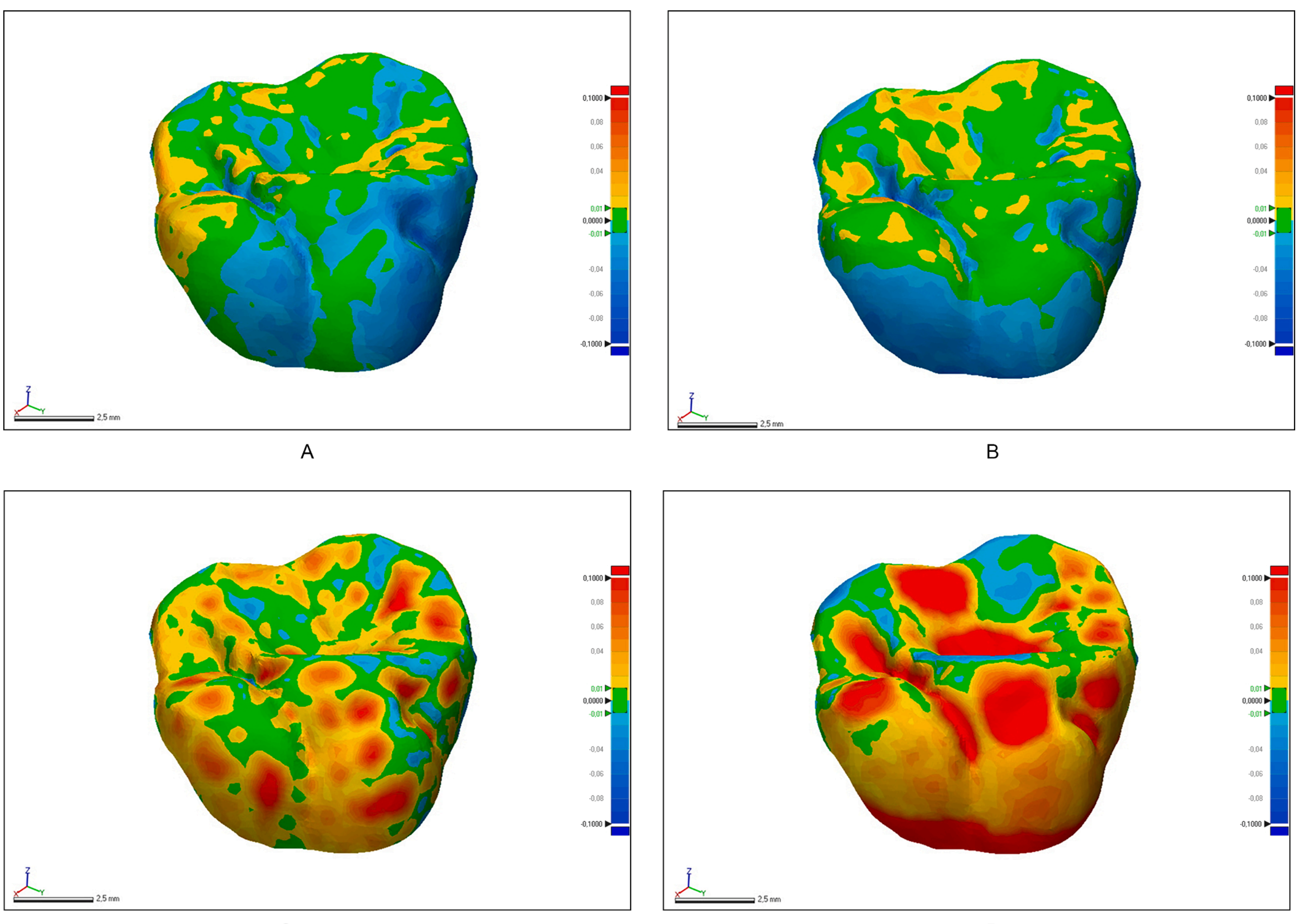

Fig. 5. Representative color map of RMS error discrepancies measured among the control subgroups tested. Data provided in millimeters (mm). Max/min nominal 10 µm (green). Max/min critical 100 µm (dark red and dark blue). A, Control-dry subgroup. B, Control-low subgroup. C, Control-Mild subgroup. D, Control-High subgroup. RMS, root mean square (For interpretation of the references to color in this figure legend, the reader is referred to the web version of this article).

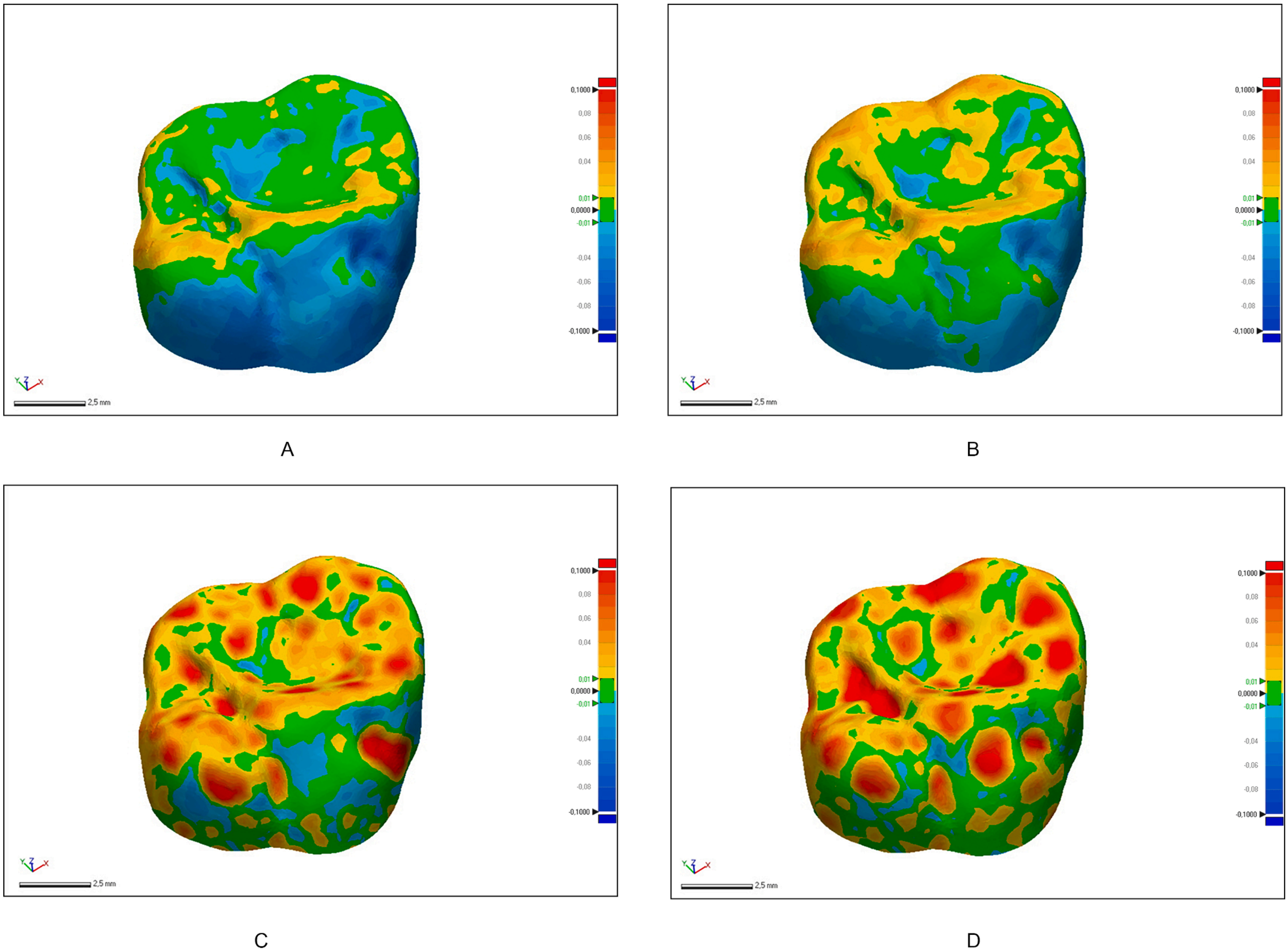

Fig. 6. Representative color map of RMS error discrepancies measured among the Z subgroups tested. Data provided in millimeters (mm). Max/min nominal 10 µm (green). Max/min critical 100 µm (dark red and dark blue). A, Z-dry subgroup. B, Z-low subgroup. C, Z-Mild subgroup. D, Z-High subgroup. RMS, root mean square; Z, Zirconia (For interpretation of the references to color in this figure legend, the reader is referred to the web version of this article).

3 different restorative materials namely zirconia (IPS e.max ZirCad, LT, A1; Ivoclar Vivadent), lithium disilicate ceramic (IPS e.max CAD, LT, A1; Ivoclar Vivadent), and a nanoceramic resin material (Grandio, LT, A1; VOCO) by using a chairside milling machine (CEREC MC XL; Dentsply Sirona) following the manufacturer's recommendations. The zirconia crown was sintered using an oven (CEREC SpeedFire; Dentsply Sirona) following the manufacturer's protocol. Afterwards, the crown was polished using specific polishing bur kit (ZiLMaster Finishing & Polishing Kit HP; Shofu). Similarly, the lithium disilicate crown was sintered using an oven (Programat p300; Ivoclar Vivadent) following the manufacturer's protocol and polished using a specific polishing bur kit (ZiLMaster Finishing & Polishing Kit HP; Shofu). Lastly, the nanoceramic crown was polished using a specific polishing bur (Set RA 341; EVE) (Fig. 3).

In the Z group, the zirconia crown was cemented in the first molar of the reference cast by using a temporary cement (NextTemp Temporary Cement, clear; Premier Dental Co.) following the manufacturer's recommendations (Fig. 4). Then, a reference scan was obtained by using the same laboratory scanner, as well as same scanning procedure as in the control reference scan. For the acquisition of the specimens of the Z-dry, Z-low, Z-mild, and Z-high subgroups, the same procedures as in the control-dry, control-low, control-mild, and control-high subgroups were respectively performed.

In the LD and NC groups, the lithium disilicate and nanoceramic crowns were respectively used in each group using the same protocol as in the Z group. Additionally, for the data acquisition of the corresponding LD and NC subgroups, the same procedures as in the control-dry, control-low, control-mild, and control-high subgroups were respectively accomplished.

The reference scan of each subgroup was used to measure the scanning discrepancies among the intraoral digital scans obtained under the different wetness conditions. Each STL file obtained in the different experimental subgroups was imported into a reverse engineering software program (Geomagic Wrap, v.2021; 3D Systems). The CAD tools were used to align each reference scan with the corresponding experimental scan using the best fit algorithm, selecting the second premolar and second molar areas. Subsequently, the root mean square (RMS) error in the maxillary first molar area was calculated (Figs. 5–8), using the following formula: $RMS = \sqrt{\frac{\sum_{i=1}^{n}(X_{1,i}-X_{2,i})^2}{n}}$, where $X_{1,i}$ are the reference data, $X_{2,i}$ are the scan data, and n indicates the total number of measurement points measured in each analysis. Trueness was defined as the closeness of agreement between the reference scan and the experimental intraoral digital scans [42,43]. Precision was described as closeness of agreement between independent results of measurement obtained under stipulated conditions, or as the variations per each subgroup or standard deviation (SD) [42,43].

The Shapiro-Wilk test revealed that the data were normally

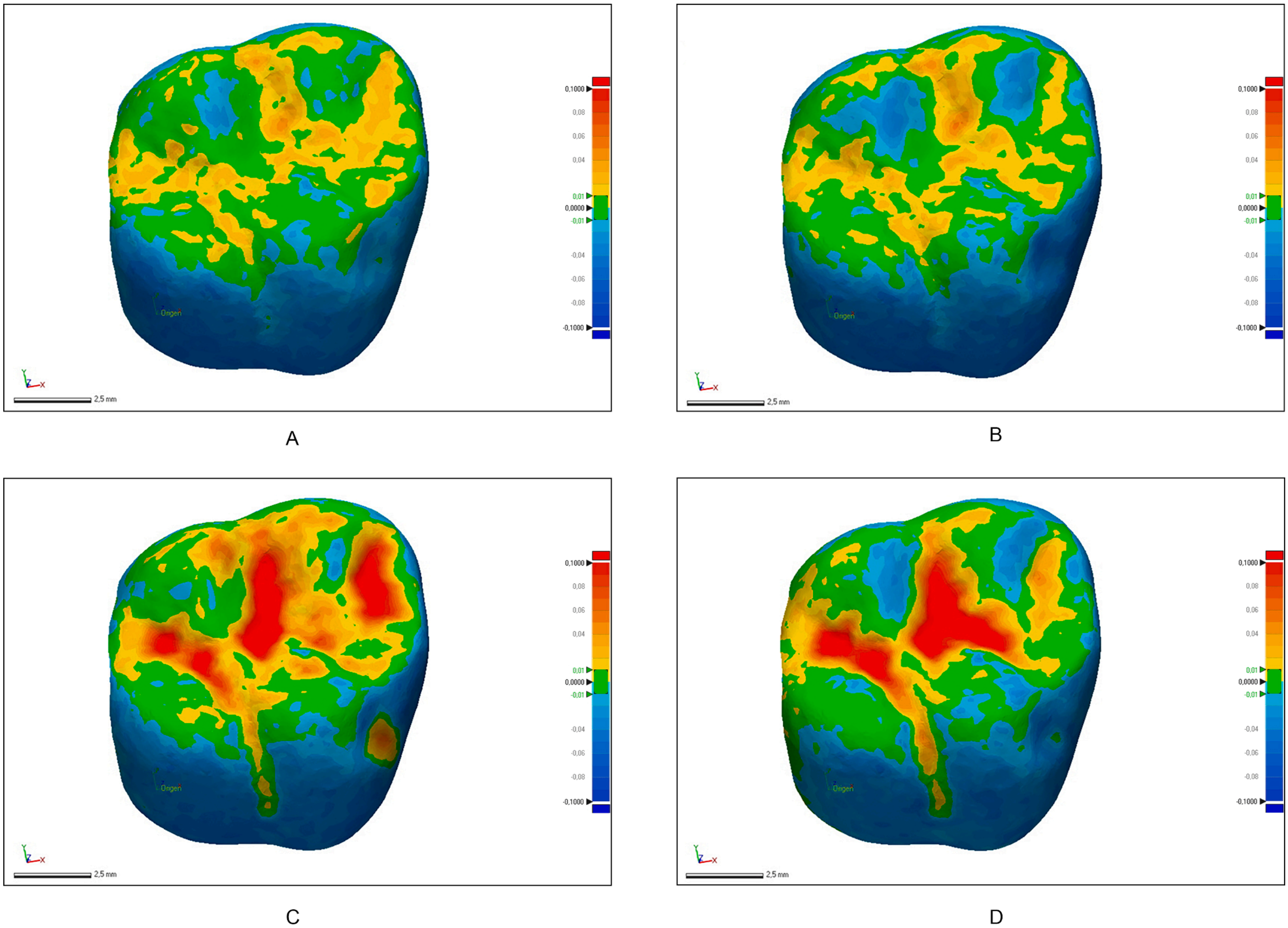

Fig. 7. Representative color map of RMS error discrepancies measured among the LD subgroups tested. Data provided in millimeters (mm). A, LD-dry subgroup. B, LD-low subgroup. C, LD-Mild subgroup. D, LD-High subgroup. LD, lithium disilicate; RMS, root mean square.

distributed (P>.05). Two-way analysis of variance (ANOVA) followed by the Bonferroni pairwise multiple comparison tests were used to analyze the trueness data (α=0.05). The Levene test followed by the Bonferroni pairwise comparison tests were used to assess precision among the subgroups tested (α=0.05). The statistical analysis was completed using a statistical software program (IBM SPSS Statistics for Windows, v26; IBM Corp).

3. Results

The mean ±SD RMS errors obtained among the subgroups tested are presented in Table 2. Regarding trueness, the 2-way ANOVA analysis of variance showed that the group or material type ($P < .001$) and subgroup or wetness of the surface being digitized ($P < .001$) were significant predictors of the intraoral scanning trueness of the IOS tested (Fig. 9). With respect to the group factor, the Bonferroni test showed significant mean trueness discrepancies between the different groups ($P < .001$) and subgroups tested ($P < .001$). Regarding the material tested, all groups under dry and low wetness conditions were not significantly different. However, the mild and high subgroups showed lower mean trueness values compared with the dry and low subgroups (Table 3). Regarding the wetness conditions tested, the control, Z, and LD groups under dry and low wetness conditions obtained significantly better mean trueness values than the NC group (Table 4). Under mild wetness conditions, all the materials revealed no significant discrepancies in the mean trueness values. Under high wetness conditions, the LD group showed the best mean trueness value, followed by the NC group, while the control (enamel) and Z groups yielded the poorest mean trueness values (Table 4).

Regarding the evaluation of precision, the Levene test showed significant differences in the SDs among the groups tested ($P < .001$) and across the subgroups ($P < .001$). Regarding the material tested, the dry and low subgroups in all groups were not significantly different. However, the mild and high subgroups revealed lower precision mean values compared with the dry and low subgroups (Table 5). In relation to the wetness conditions tested, under dry and low wetness conditions, all the materials showed no significant precision discrepancies (Table 6). Under mild wetness conditions, the LD and NC groups yielded significantly better precision mean values compared with the control and Z groups. Under high wetness conditions, the LD group obtained the best precision mean value among the groups tested.

4. Discussion

Based on the results of the present study, the humidity conditions and the material type of the surface being scanned impacted scanning trueness and precision values of the IOS tested. Therefore, the null hypothesis was rejected. The scanning trueness values ranged from 22 to 61 μm, while the scanning precision values ranged from 1 to 13 μm. The scanning accuracy discrepancies measured among the different groups were relatively low but could have a variable clinical impact depending on the purpose of the intraoral digital scan (diagnostic or definitive

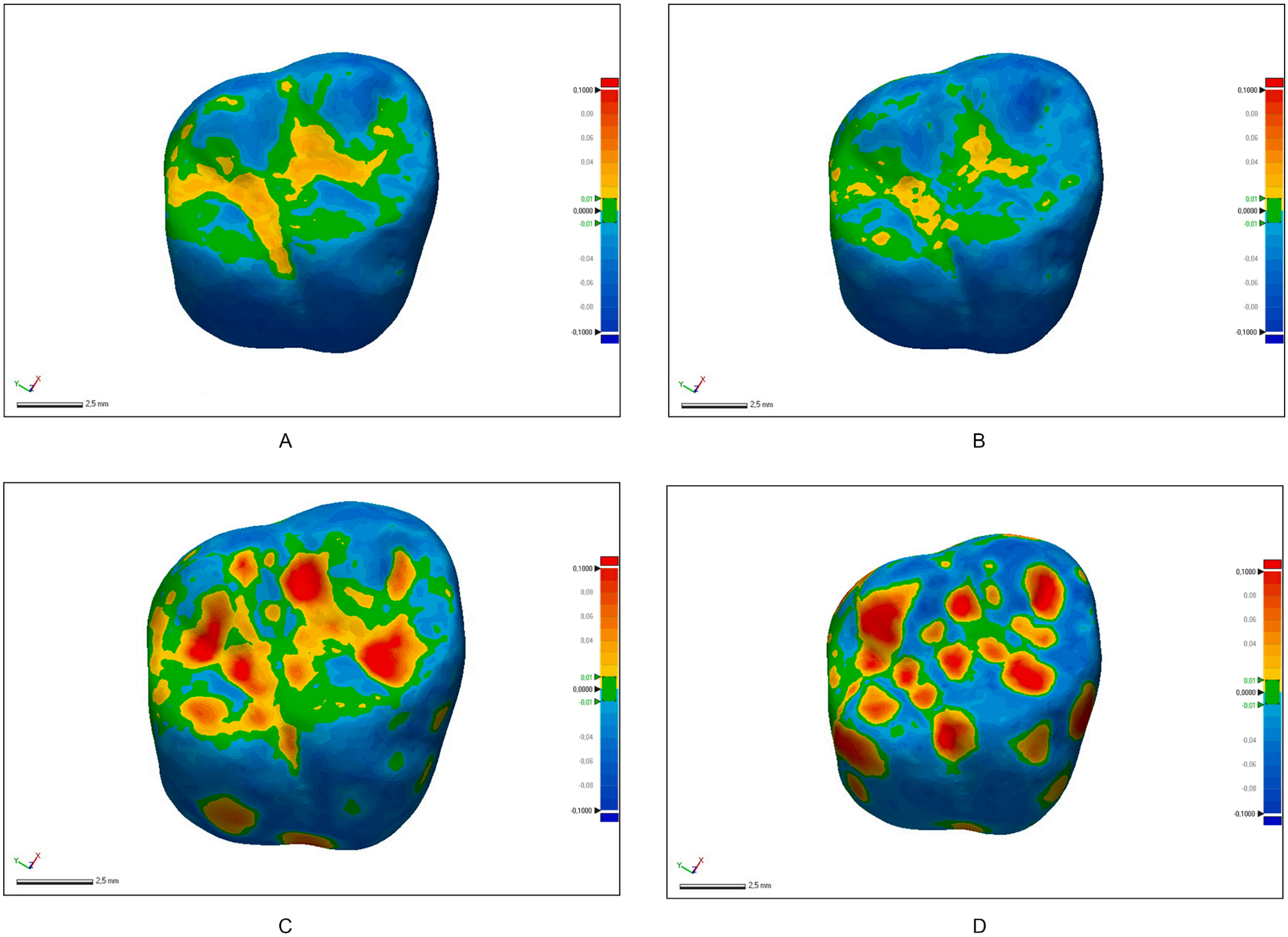

Fig. 8. Representative color map of RMS error discrepancies measured among the NC subgroups tested. Data provided in millimeters (mm). A, NC-dry subgroup. B, NC-low subgroup. C, NC-Mild subgroup. D, NC—High subgroup. RMS, root mean square.

Table 2
Trueness and precision values obtained among the different subgroups tested.

Group	Subgroup	Trueness (mean RMS error) (mm)	Precision (SD) (mm)
Control	Dry	0.022	0.002
	Low	0.023	0.002
	Mild	0.034	0.008
	High	0.061	0.013
Z	Dry	0.022	0.002
	Low	0.023	0.001
	Mild	0.032	0.005
	High	0.056	0.015
LD	Dry	0.025	0.001
	Low	0.027	0.002
	Mild	0.033	0.002
	High	0.032	0.004
NC	Dry	0.036	0.001
	Low	0.034	0.002
	Mild	0.034	0.004
	High	0.052	0.012

LD, lithium disilicate; NC, nanoceramic resin; Z, zirconia.

cast). Further studies are needed to assess the clinical implications of the scanning accuracy discrepancies based on the clinical purpose of the intraoral digital scan.

Similarly, as in conventional methods, definitive casts require higher accuracy than diagnostic casts. The scanning discrepancies recorded as consequence of wetness and existing restorative materials in the patient's dentition may have greater impact when acquiring virtual definitive casts when compared with diagnostic casts. In this context, having an existing restoration adjacent to a tooth preparation or an implant scan body may influence on the accuracy on the proximal contacts of the definitive restoration. Similarly, if the existing restoration is present in the antagonist dentition, it is unclear how the scanning discrepancies measured in this study might impact upon the maxillo-mandibular relationship or the occlusal surface of the definitive restoration fabricated by using a complete digital workflow. Additional investigations are needed to assess the clinical impact of the scanning discrepancies captured in an intraoral digital scan among patients with existing restorations and the presence of wetness on the surface being digitized.

In the present investigation, the control and Z groups under dry and low-wetness conditions obtained similar trueness and precision mean values of the IOS tested. Additionally, these groups under the mild and high wetness conditions demonstrated lower scanning accuracy values compared with the dry and low wetness settings. Dry polished zirconia seems to present reflectance characteristics similar to those of natural human enamel. However, previous literature has demonstrated the influence of ceramic translucency on intraoral scanning accuracy [24]. In the present study, a low translucency zirconia material with color A1 was selected. Generalization of the results of this study should be made with caution.

The results of this study revealed that, overall, the greater the wetness of the surface being digitized, the lower the scanning accuracy

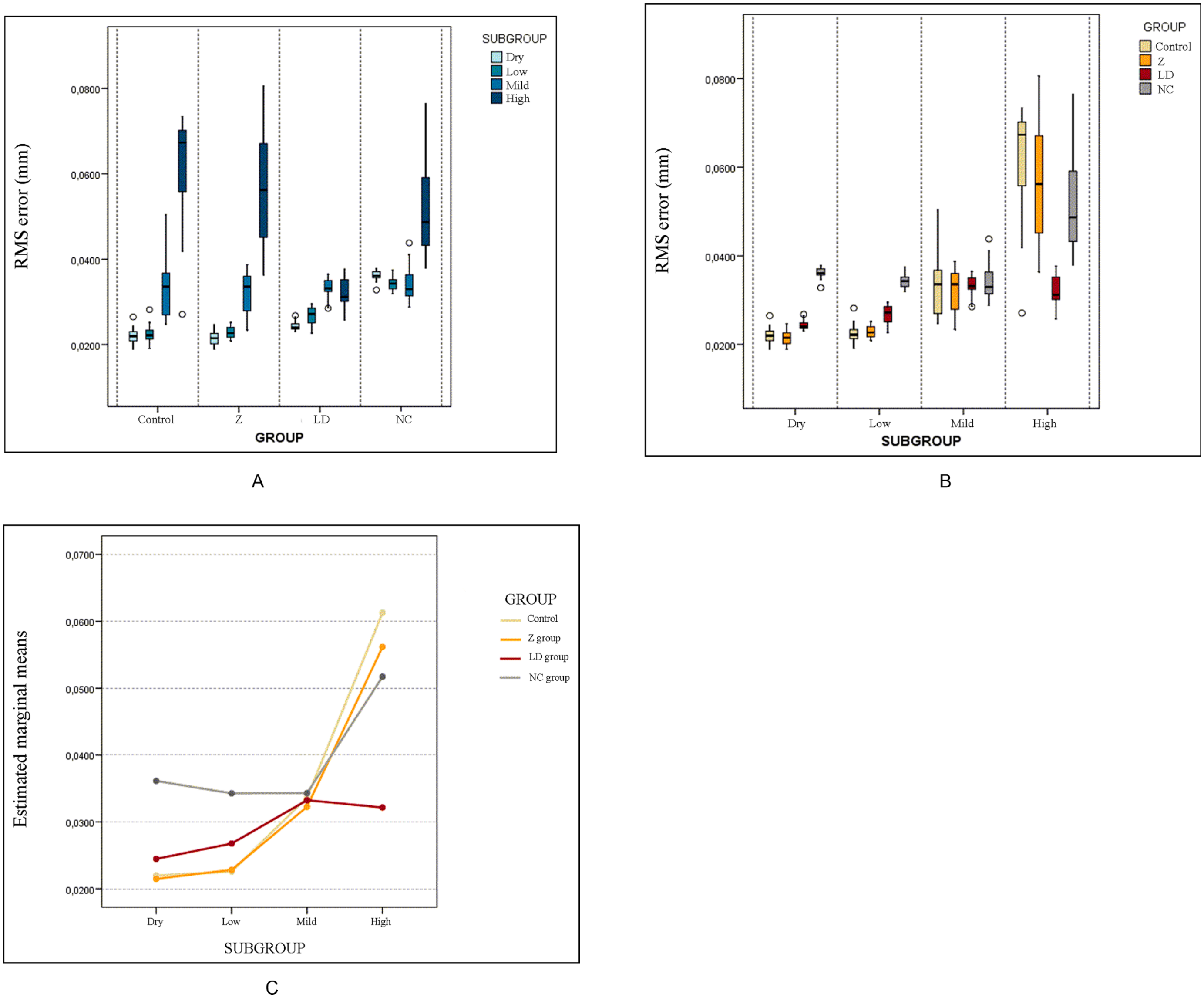

Fig. 9. A, Boxplot of the RMS error values measured by subgroup. B, Boxplot of the RMS error values measured by subgroup C, Estimated marginal means graphic for the different subgroups tested. LD, lithium disilicate; NC, nanoceramic resin; RMS, root mean square; Z, zirconia.

values obtained. However, under mild wetness conditions, the materials tested showed no significant discrepancies in the mean trueness values of the IOS tested. Nevertheless, the LD and NC groups exhibited significantly better precision mean values compared with the control and Z groups. Additionally, under high wetness conditions, the lithium disilicate material tested obtained the best trueness and precision mean values among the different study groups. These findings confirm the different effect of the restorative dental materials and the wetness characteristics of the surface being digitized on intraoral scanning accuracy. Clinically, it may be advisable for the surface being digitized to be as dry as possible, in order to maximize performance of the IOS tested.

The presence of existing restorative material in the dentition being digitized has been reported as a factor that can reduce the scanning accuracy of IOSs [35,36]. A previous in vitro study revealed that the influence of the restorative materials on the accuracy values varied depending on the IOS technology and system selected [35]. In this previous study, the authors tested 8 different IOSs involving the Trios 3 and 14 different dry substrate materials, including enamel, zirconia, and lithium disilicate ceramic. In the case of the dry enamel evaluation using the Trios 3, the authors reported a trueness value of 25 ± 20 μm and a precision value of 36 ± 28 μm. In the present investigation, the dry enamel group obtained better trueness and precision values. This might be explained by variations in the geometries of the specimens tested and software version discrepancies of the Trios 3 used. The zirconia (IPS e.max ZirCad; Ivoclar Vivadent) and lithium disilicate ceramic (IPS e.max CAD; Ivoclar Vivadent) materials tested were the same materials as those used in this present study; however, the color and surface finishing selected for the zirconia material were not disclosed. In the case of the lithium disilicate ceramic, the authors used MT (medium translucency) and A2 color, while in the present investigation LT (low translucency) and A1 lithium disilicate material were tested. In relation to the Trios 3, the authors reported a trueness value of 22 ± 6 μm and precision value of 31 ± 8 μm for the zirconia group and a trueness value of 24 ± 14 μm and precision value of 34 ± 20 μm for the lithium disilicate group. These results are consistent with the trueness values obtained in the present study; however, better precision mean values have been obtained in this investigation. This might be explained by discrepancies in the translucency, color, surface finishing, and geometry of the specimens used, as well as by the different IOS software version of the Trios 3 involved.

A previous in vitro study assessed the influence of different dry restorative materials including zirconia, lithium disilicate ceramic, and

Table 3
Bonferroni multiple pairwise comparison trueness values obtained in each group.

Group	Subgroup	Dry	1 ml/min	4 ml/min
Control	Dry [a]			
	Low [a]	1.000		
	Mild [b]	<0.001***	<0.001***	
	High [c]	<0.001***	<0.001***	<0.001***
Z	Dry [a]			
	Low [a]	1.000		
	Mild [b]	<0.001***	.001**	
	High [c]	<0.001***	<0.001***	<0.001***
LD	Dry [a]			
	Low [ac]	1.000		
	Mild [b]	.002**	.040*	
	High [bc]	.008**	.142	1.000
NC	Dry [a]			
	Low [a]	1.000		
	Mild [a]	1.000	1.000	
	High [b]	<0.001***	<0.001***	<0.001***

LD, lithium disilicate; NC, nanoceramic resin; Z, zirconia
In each group, subgroups with the same superscript indicate no significant difference.

Table 4
Bonferroni multiple pairwise comparison trueness values obtained in each subgroup.

Subgroup	Group	Control	Z	LD
Dry	Control [a]			
	Z [a]	1.000		
	LD [a]	1.000	1.000	
	NC [b]	<0.001***	<0.001***	<0.001***
Low	Control [a]			
	Z [a]	1.000		
	LD [a]	.457	.586	
	NC [b]	<0.001***	<0.001***	.010*
Mild	Control [a]			
	Z [a]	1.000		
	LD [a]	1.000	1.000	
	NC [a]	1.000	1.000	1.000
High	Control [a]			
	Z [ab]	.193		
	LD [c]	<0.001***	<0.001***	
	NC [b]	<0.001***	.366	<0.001***

LD, lithium disilicate; NC, nanoceramic resin; Z, zirconia
In each subgroup, groups with the same superscript indicate no significant difference.

Table 5
Bonferroni multiple pairwise comparison precision values obtained in each group.

Group	Subgroup	Dry	Low	Mild
Control	Dry [a]			
	Low [a]	1.000		
	Mild [b]	.018*	.024*	
	High [b]	.002**	.002**	.516
Z	Dry [a]			
	Low [a]	1.000		
	Mild [b]	.002**	.001**	
	High [c]	<0.001***	<0.001***	.002**
LD	Dry [a]			
	Low [ab]	.162		
	Mild [ab]	.396	1.000	
	High [bc]	.006**	.258	.576
NC	Dry [a]			
	Low [a]	1000		
	Mild [b]	0,006**	.024*	
	High [c]	<0,001***	<0.001***	.012*

LD, lithium disilicate; NC, nanoceramic resin; Z, zirconia
In each subgroup, groups with the same superscript indicate no significant difference.

Table 6
Bonferroni multiple pairwise comparison precision values obtained in each subgroup.

Subgroup	Groups	Control	Z	LD
Dry	Control [a]			
	Z [a]	1.000		
	LD [a]	.924	1.000	
	NC [a]	1.000	1.000	1.000
Low	Control [a]			
	Z [a]	1.000		
	LD [a]	1.000	1.000	
	NC [a]	1.000	1.000	1.000
Mild	Control [a]			
	Z [a]	1.000		
	LD [bc]	.036*	.030*	
	NC [ac]	.684	1.000	.180
High	Control [a]			
	Z [a]	1.000		
	LD [b]	.012*	<0.001***	
	NC [a]	1.000	1.000	.006**

LD, lithium disilicate; NC, nanoceramic resin; Z, zirconia
In each group, subgroups with the same superscript indicate no significant difference.

nanoceramic composite resin material on the scanning accuracy of an IOS (Trios 4; 3Shape A/S). Additionally, 2 different surface finishings were considered namely polished and glazed. Results revealed that polished restorations yielded lower scanning discrepancies when compared with glazed restorations, except for the zirconia material tested (LAVA Plus, A2; 3M ESPE) [36]. The authors reported a mean trueness value of 25 µm and a mean precision value of 1 µm for the polished zirconia, a mean trueness value of 23 µm and a mean precision value of 1 µm for the polished lithium disilicate ceramic, and a mean trueness value of 32 µm and a mean precision value of 1 µm for the polished nanoceramic composite resin. In the present study, all the specimens were polished aiming to standardize the surface finish among the materials tested. Although a different IOS generation was selected in this study, similar accuracy values for the dry polished zirconia, lithium disilicate ceramic, and nanoceramic composite resin materials.

Previous studies have described the influence of the wetness of the surface being digitized on intraoral scanning accuracy [37,38,41]. However, none of them attempted to simulate different degrees of surface wetness.

In an in vitro setting, Chen et al. [37] evaluated the influence of wetness (dry, wet, and blow-dried) on the accuracy of 2 IOSs (Trios 3 from 3Shape and PrimeScan from Dentsply Sirona). The wet condition was obtained by completely submerging the typodont in a container with artificial saliva, followed by subsequent removal of the liquid of the container leaving the typodont with a wet surface. The authors reported the lowest complete-arch scanning accuracy values in the wet condition groups. Comparisons with the results of this study are challenging, due to differences in the wetness characteristics of the surface being scanned, materials tested, and measurement methods employed.

A previous clinical investigation evaluated the effect of saliva isolation and ambient lighting conditions on intraoral scanning accuracy of an IOS (Trios from 3Shape A/S) [38]. The authors reported no statistically significant difference among the groups tested. Similarly, a previous in vitro study assessed the influence of orthodontic brackets and artificial saliva on the accuracy of 4 IOSs including the Trios 3. Artificial saliva was applied using an art brush onto the surface of the typodont, with three pumps for each application. More artificial saliva was applied before the moisture dried up. The authors described between 2 and 3 applications for each scanning set (10-time scan for each scanner) [38]. Comparisons with the results present investigation is not feasible due to research methodology discrepancies among these studies.

The present investigation has several limitations, such as the laboratory settings, the fact that only one IOS was used, and the restricted assessment of restorative materials. Furthermore, scanning time was not considered a variable of this study. Additional laboratory and clinical studies are recommended to further evaluate the influence of the wetness characteristics of the surface being digitized and the different restorative materials with variable colors and translucencies on the scanning accuracy of different IOSs.

5. Conclusions

Based on the findings of the present in vitro study, the following conclusions were drawn:

- The different restorative materials and wetness characteristics of the surface being digitized influenced scanning trueness and precision of the IOS assessed.
- Overall, the higher the wetness characteristics of the surface being digitized, the lower the scanning trueness and precision values measured.
- Under all the wetness conditions, the control (enamel) and polished zirconia specimens yielded similar trueness and precision mean values of the IOS tested. Additionally, under the mild and high wetness conditions, these groups demonstrated lower scanning accuracy values compared with the dry and low wetness settings.
- Under mild wetness conditions, the materials tested showed no significant discrepancies in trueness values. However, the LD and NC groups yielded significantly better precision mean values compared with the control and Z groups.
- Under high wetness conditions, the lithium disilicate material yielded the best trueness and precision mean values among the groups tested.

Credit author statement

Rubén Agustín-Panadero: Contributed to protocol development, IRB submission, data collection, results interpretation, and revision of the manuscript.

David Macías Moreno: Data collection.

Jorge Alonso Pérez-Barquero: Contributed to the protocol development, IRB submission, and performed data measurements.

Lucía Fernández-Estevan: Contributed to data collection revisions, data analysis, results interpretation, and revision of the manuscript.

Miguel Gómez-Polo: Contributed to protocol development, results interpretation, and revision of the manuscript.

Marta Revilla-León: Contributed to protocol development, results interpretation, and manuscript writing.

All authors discussed the evolution and commented on the manuscript at all stages

Funding

This research did not receive any specific grant from funding agencies in the public, commercial, or not-for-profit sectors.

Declaration of Competing Interest

The authors did not have any conflict of interest, financial or personal, in any of the materials described in this study.

References

[1] M. Revilla-León, K. Frazier, J.B. da Costa, P. Kumar, M.L. Duong, S. Khajotia, et al., Council on scientific affairs. intraoral scanners: an american dental association clinical evaluators panel survey, J. Am. Dent. Assoc. 152 (2021) 669–670, https://doi.org/10.1016/j.adaj.2021.05.018.
[2] M Gómez-Polo, A Sallorenzo, R Ortega, C Gómez-Polo, AB Barmak, W Att, M Revilla-León, Influence of implant angulation and clinical implant scan body height on the accuracy of complete arch intraoral digital scans, J. Prosthet. Dent. (2022), https://doi.org/10.1016/j.prosdent.2021.11.018.
[3] L. Giachetti, C. Sarti, F. Cinelli, D.S. Russo, Accuracy of digital impressions in fixed prosthodontics: a systematic review of clinical studies, Int. J. Prosthodont. 33 (2020) 192–201, https://doi.org/10.11607/ijp.6468.
[4] M. Tabesh, F. Nejatidanesh, G. Savabi, A. Davoudi, O. Savabi, H. Mirmohammadi, Marginal adaptation of zirconia complete-coverage fixed dental restorations made from digital scans or conventional impressions: a systematic review and meta-analysis, J. Prosthet. Dent. 125 (2021) 603–610, https://doi.org/10.1016/j.prosdent.2020.01.035.
[5] K. Chochlidakis, P. Papaspyridakos, A. Tsigarida, D. Romeo, Y.W. Chen, Z. Natto, C. Ercoli, Digital versus conventional full-arch implant impressions: a prospective study on 16 edentulous maxillae, J. Prosthodont. 29 (2020) 281–286, https://doi.org/10.1111/jopr.13162.
[6] C. Wulfman, A. Naveau, C. Rignon-Bret, Digital scanning for complete-arch implant-supported restorations: a systematic review, J. Prosthet. Dent. 124 (2020) 161–167, https://doi.org/10.1016/j.prosdent.2019.06.014.
[7] M. Revilla-León, D.E. Kois, J.C. Kois, A guide for maximizing the accuracy of intraoral digital scans. Part 1: operator factors, J. Esthet. Restor. Dent. (2022) [Epub ahead of print].
[8] M. Revilla-León, D.E. Kois, J.C. Kois, A guide for maximizing the accuracy of intraoral digital scans. Part 2: patient factors, J. Esthet. Restor. Dent. (2022) [Epub ahead of print].
[9] P. Medina-Sotomayor, A. Pascual-Moscardó, I. Camps, Relationship between resolution and accuracy of four intraoral scanners in complete-arch impressions, J. Clin. Exp. Dent. 10 (2018) e361–e366, https://doi.org/10.4317/jced.54670.
[10] M. Revilla-León, A. Gohil, A.B. Barmak, M. Gómez-Polo, J.A. Pérez-Barquero, W. Att, J.C. Kois, Influence of ambient temperature changes on intraoral scanning accuracy, J. Prosthet. Dent. (2022), https://doi.org/10.1016/j.prosdent.2022.01.012 [Epub ahead of print].
[11] W. Renne, M. Ludlow, J. Fryml, Z. Schurch, A. Mennito, R. Kessler, A. Lauer, Evaluation of the accuracy of 7 digital scanners: an in vitro analysis based on 3-dimensional comparisons, J. Prosthet. Dent. 118 (2017) 36–42, https://doi.org/10.1016/j.prosdent.2016.09.024.
[12] K.C. Oh, J.M. Park, H.S. Moon, Effects of scanning strategy and scanner type on the accuracy of intraoral scans: a new approach for assessing the accuracy of scanned data, J. Prosthodont. 29 (2020) 518–523, https://doi.org/10.1111/jopr.13158.
[13] P. Müller, A. Ender, T. Joda, J. Katsoulis, Impact of digital intraoral scan strategies on the impression accuracy using the TRIOS Pod scanner, Quintessence Int. 47 (2016) 343–349, https://doi.org/10.3290/j.qi.a35524.
[14] Y.G. Moon, K.M. Lee, Comparison of the accuracy of intraoral scans between complete-arch scan and quadrant scan, Prog. Orthod. 21 (2020) 36, https://doi.org/10.1186/s40510-020-00337-1.
[15] M.K. Kim, K. Son, B.Y. Yu, K.B. Lee, Effect of the volumetric dimensions of a complete arch on the accuracy of scanners, J. Adv. Prosthodont. 12 (2020) 361–368, https://doi.org/10.4047/jap.2020.12.6.361.
[16] J.H. Lim, J.M. Park, M. Kim, S.J. Heo, J.Y. Myung, Comparison of digital intraoral scanner reproducibility and image trueness considering repetitive experience, J. Prosthet. Dent. 119 (2018) 225–232, https://doi.org/10.1016/j.prosdent.2017.05.002.
[17] J. Kim, J.M. Park, M. Kim, S.J. Heo, I.H. Shin, M. Kim, et al., Comparison of experience curves between two 3-dimensional intraoral scanners, J. Prosthet. Dent. 116 (2016) 221–230, https://doi.org/10.1016/j.prosdent.2015.12.018.
[18] M. Revilla-León, P. Jiang, M. Sadeghpour, W. Piedra-Cascón, A. Zandinejad, M. Özcan, V.R. Krishnamurthy, Intraoral digital scans-Part 1: influence of ambient scanning light conditions on the accuracy (trueness and precision) of different intraoral scanners, J. Prosthet. Dent. 124 (2020) 372–378, https://doi.org/10.1016/j.prosdent.2019.06.003.
[19] M. Revilla-León, P. Jiang, M. Sadeghpour, W. Piedra-Cascón, A. Zandinejad, M. Özcan, V.R. Krishnamurthy, Intraoral digital scans: part 2-influence of ambient scanning light conditions on the mesh quality of different intraoral scanners, J. Prosthet. Dent. 124 (2020) 575–580, https://doi.org/10.1016/j.prosdent.2019.06.004.
[20] M. Revilla-León, S.G. Subramanian, M. Özcan, V.R. Krishnamurthy, Clinical study of the influence of ambient light scanning conditions on the accuracy (trueness and precision) of an intraoral scanner, J. Prosthodont. 29 (2020) 107–113, https://doi.org/10.1111/jopr.13135.
[21] M. Revilla-León, S.G. Subramanian, W. Att, V.R. Krishnamurthy, Analysis of different illuminance of the room lighting condition on the accuracy (trueness and precision) of an intraoral scanner, J. Prosthodont. 30 (2021) 157–162, https://doi.org/10.1111/jopr.13135.
[22] R. Jin-Young Kim, G.I. Benic, J.M. Park, Trueness of intraoral scanners in digitizing specific locations at the margin and intaglio surfaces of intracoronal preparations, J. Prosthet. Dent. (2020), https://doi.org/10.1016/j.prosdent.2020.09.019. Epub ahead of print.
[23] J.W. Anh, J.M. Park, Y.S. Chun, M. Kim, M. Kim, A comparison of the precision of three-dimensional images acquired by 2 digital intraoral scanners: effects of tooth irregularity and scanning direction, Korean J. Orthod. 46 (2016) 3–12, https://doi.org/10.4041/kjod.2016.46.1.3.
[24] H. Li, P. Lyu, Y. Wang, Y. Sun, Influence of object translucency on the scanning accuracy of a powder-free intraoral scanner: a laboratory study, J. Prosthet.Dent. 117 (2017) 93–101, https://doi.org/10.1016/j.prosdent.2016.04.008.
[25] M. Gómez-Polo, W. Piedra-Cascón, M.M. Methani, N. Quesada-Olmo, M. Farjas-Abadía, M. Revilla-León, Influence of rescanning mesh holes and stitching

procedures on the complete-arch scanning accuracy of an intraoral scanner: an in vitro study, J. Dent. 110 (2021), 103690, https://doi.org/10.1016/j.jdent.2021.103690.
[26] M. Revilla-León, E. Sicilia, R. Agustín-Panadero, M. Gómez-Polo, J.C. Kois, Clinical evaluation of the effects of cutting off, overlapping, and rescanning procedures on intraoral scanning accuracy, J. Prosthet. Dent. (2022), https://doi.org/10.1016/j.prosdent.2021.10.017 [Epub ahead of print].
[27] R.M. Mizumoto, B. Yilmaz, Intraoral scan bodies in implant dentistry: a systematic review, J. Prosthet. Dent. 120 (2018) 343–352, https://doi.org/10.1016/j.prosdent.2017.10.029.
[28] M. Moslemion, L. Payaminia, H. Jalali, M. Alikhasi, Do type and shape of scan bodies affect accuracy and time of digital implant impressions? Eur. J. Prosthodont. Restor. Dent. 28 (2020) 18–27, https://doi.org/10.1922/EJPRD_1962Moslemion10.
[29] L. Arcuri, A. Pozzi, F. Lio, E. Rompen, W. Zechner, A. Nardi, Influence of implant scanbody material, position and operator on the accuracy of digital impression for complete-arch: a randomized in vitro trial, J. Prosthodont. Res. 64 (2020) 128–136, https://doi.org/10.1016/j.jpor.2019.06.001.
[30] K. Basaki, H. Alkumru, G. De Souza, Y. Finer, Accuracy of digital vs conventional implant impression approach: a three-dimensional comparative in vitro analysis, Int. J. Oral Maxillofac. Implants. 32 (2017) 792–799, https://doi.org/10.11607/jomi.5431.
[31] A.L. Carneiro Pereira, V.R. Medeiros, A. da Fonte Porto Carreiro, Influence of implant position on the accuracy of intraoral scanning in fully edentulous arches: a systematic review, J. Prosthet. Dent. (2020), https://doi.org/10.1016/j.prosdent.2020.09.008 [Epub ahead of print].
[32] W.S. Lin, B.T. Harris, E.N. Elathamna, T. Abdel-Azim, D. Morton, Effect of implant divergence on the accuracy of definitive casts created from traditional and digital implant-level impressions: an in vitro comparative study, Int. J. Oral Maxillofac. Implants. 30 (2015) 102–109, https://doi.org/10.11607/jomi.3592.
[33] Y.J. Zhang, J.Y. Shi, S.J. Qian, S.C. Qiao, H.C. Lai, Accuracy of full-arch digital implant impressions taken using intraoral scanners and related variables: a systematic review, Int. J. Oral Implantol. 14 (2021) 157–179, https://doi.org/10.1016/j.prosdent.2020.04.004 (Berl).
[34] Y.D. Choi, K.E. Lee, H.N. Mai, D.H. Lee, Effects of scan body exposure and operator on the accuracy of image matching of implant impressions with scan bodies, J. Prosthet. Dent. 124 (2020), https://doi.org/10.1016/j.prosdent.2020.04.004, 379.e1-6.
[35] E. Dutton, M. Ludlow, A. Mennito, A. Kelly, Z. Evans, A. Culp, R. Kessler, W. Renne, The effect different substrates have on the trueness and precision of eight different intraoral scanners, J. Esthet. Restor. Dent. 2 (2020) 204–218, https://doi.org/10.1111/jerd.12528.
[36] M. Revilla-León, K. Young, E. Sicilia, S.H. Cho, J.C. Kois, Influence of definitive and interim restorative materials and surface finishing on the scanning accuracy of an intraoral scanner, J. Dent. 120 (2022), 104114, https://doi.org/10.1016/j.jdent.2022.104114.
[37] Y. Chen, Z. Zhai, H. Li, S. Yamada, T. Matsuoka, S. Ono, T. Nakano, Influence of liquid on the tooth surface on the accuracy of intraoral scanners: an *in vitro* study, J. Prosthodont. (2021), https://doi.org/10.1111/jopr.13358 [Epub ahead of print].
[38] H. Camci, F. Salmanpour, Effect of saliva isolation and intraoral light levels on performance of intraoral scanners, Am. J. Orthod. Dentofac. Orthop. 158 (2020) 759–766, https://doi.org/10.1016/j.ajodo.2020.03.022.
[39] H.N. Park, Y.J. Lim, W.J. Yi, J.S. Han, S.P. Lee, A comparison of the accuracy of intraoral scanners using an intraoral environment simulator, J. Adv. Prosthodont. 10 (2018) 58–64, https://doi.org/10.4047/jap.2018.10.1.58.
[40] M. Gómez-Polo, R. Ortega, A. Sallorenzo, R. Agustín-Panadero, A.B. Barmak, J. C. Kois, M. Revilla-León, Influence of the surface humidity, implant angulation, and interimplant distance on the accuracy and scanning time of complete-arch implant scans, J. Dent. 127 (2022), 104307, https://doi.org/10.1016/j.jdent.2022.104307.
[41] J. Song, M. Kim, Accuracy on scanned images of full arch models with orthodontic brackets by various intraoral scanners in the presence of artificial saliva, Biomed. Res. Int. 27 (2020), 2920804, https://doi.org/10.1155/2020/2920804.
[42] International Organization for Standardization. ISO 5725-1:1994. Accuracy (trueness and precision) of measurement methods and results - Part 1: general principles and definitions. https://www.iso.org/obp/ui/#iso:std:iso:5725:-1:ed-1:v1:en Accessed 02-01-20.
[43] International Organization for Standardization. ISO 20896-1:2019. Dentistry — Digital impression devices — Part 1: Methods for assessing accuracy. https://www.iso.org/standard/69402.html Accessed 02-01-20.